European Journal of Pharmaceutics and Biopharmaceutics 177 (2022) 61–67

Contents lists available at ScienceDirect

European Journal of Pharmaceutics and Biopharmaceutics

journal homepage: www.elsevier.com/locate/ejpb

Preclinical safety of negatively charged microspheres (NCMs): Optimization of radiolabeling for *in vivo* and *ex vivo* biodistribution studies after topical administration on full-thickness wounds in a rat model

María Collantes [a,b,c,d,*], Claudia Vairo [e], Álvaro Erhard [a,b,c,1], Cristina Navas [a], Silvia Villullas [e,2], Margarita Ecay [a,b,c], Félix Pareja [c], Gemma Quincoces [b,c,d], Garazi Gainza [e,*], Iván Peñuelas [a,b,c,d]

[a] Translational Molecular Imaging Unit (UNIMTRA), Clínica Universidad de Navarra, Avenida Pío XII, 31080 Pamplona, Spain
[b] RADIOMIN Research Group, Radiopharmacy Unit, Clínica Universidad de Navarra, Avenida Pío XII, 31080 Pamplona, Spain
[c] Nuclear Medicine Department, Clínica Universidad de Navarra, Avenida Pío XII, 31080 Pamplona, Spain
[d] Instituto de Investigación Sanitaria de Navarra (IdiSNA), Spain
[e] BioKeralty Research Institute AIE, Albert Einstein, 25-E3, 01510 Miñano, Spain

ARTICLE INFO

Keywords:
Negatively charged microspheres
Wound
Topical administration
Radiolabeling
Technetium-99m
Biodistribution

ABSTRACT

Negatively charged microspheres (NCMs) are postulated as a new form of treatment for chronic wounds. Despite the efficacy shown at clinical level, more studies are required to demonstrate their safety and local effect. The objective of the work was to confirm the lack of NCM systemic absorption performing a biodistribution study of the NCMs in an open wound rat animal model. To this end, radiolabeling of NCMs with technetium-99 m was optimized and biodistribution studies were performed by *in vivo* SPEC/CT imaging and *ex vivo* counting during 24 h after topical administration. The studies were performed on animals treated with a single or repeated dose to study the effect of macrophages during a prolonged treatment. NCM radiolabeling was achieved in a simple, efficient and stable manner with high yield. SPECT/CT images showed that almost all NCMs (about 85 %) remained on the wound for 24 h either after single or multiple administrations. *Ex vivo* biodistribution studies confirmed that there was no accumulation of NCMs in any organ or tissue except in the wound area, suggesting a lack of absorption. In conclusion, NCMs can be considered safe as local wound treatment since they remain at the administration area.

1. Introduction

The skin represents the largest external organ of the body whose key roles include protection against outside pathogens and excessive water loss. Wounds are injuries that break the skin barrier and can be repaired by wound healing in a complex process that involves homeostasis, inflammatory and remodeling processes and the migration and proliferation of different cell types [1]. Chronic and hard-to-heal wounds are those in which the healing process does not progress normally and remain unhealed for several weeks [2]. These types of injuries have serious consequences for patient quality of life, which include loss of mobility, difficulty in carrying out daily activities and dependency. This scenario generates a significant burden to the healthcare system. In addition, the growing aging population worldwide, the rise of chronic diseases such as diabetes (closely related with healing disorders), and the significant increase of resistance of multiple pathogens to currently existing antibiotics, make the efficient care of wounds and the search for new healing strategies a matter of great importance [3,4].

Abbreviations: NCMs, Negatively Charged Microspheres; [^{99m}Tc]TcO_4, Technetium 99mTc pertechnetate; TLC, Thin Layer Chromatography; ^{99m}Tc-NCMs, ^{99m}Tc radiolabeled NCMs; DTPA, Diethylenetriaminepentaacetic acid; $SnCl_2$, Stannous chloride; SPECT, Single Photon Emission Computed Tomography; SPECT/CT, Hybrid SPECT equipment combined with computed tomography; VOIs, Volumes of Interest.

* Corresponding authors.
E-mail addresses: mcollant@unav.es (M. Collantes), garazi.gainza@keralty.com (G. Gainza).
[1] Present address: Centro Nacional de Aceleradores, Departamento de Radiofarmacia, 41092 Sevilla, Spain.
[2] Present address: Instituto de Investigación Sanitaria Bioaraba, Vitoria, Spain.

https://doi.org/10.1016/j.ejpb.2022.06.001
Received 8 September 2021; Received in revised form 1 June 2022; Accepted 4 June 2022
Available online 11 June 2022

In this context, biomaterials and systems such as liposomes, nanoparticles, microparticles or scaffolds can help treat this type of wound. In addition to including bioactive molecules, these products can provide by themselves a suitable surface where cells involved in the healing process can attach. This union helps organize tissue reconstruction and modulate the immune and inflammatory response in the wound [5,6].

Among these new treatments, negatively charged microspheres (NCMs) appear to be a helpful and cost-effective treatment for reactivating the healing process. This technology is based on use of polystyrene NCMs (~5 μm) that carry sulfonate groups on their surface. Polystyrene possesses physical–chemical properties suitable for cell attachment, migration and proliferation [7]. *In vitro* studies have demonstrated that the increase of sulfonation and therefore the negative charge in this material leads to an increase in the number of cells attached on its surface and also the cell proliferation [8].

Recently, *in vitro* studies with NCMs have demonstrated that they possess excellent cell-adhesive properties in human fibroblast and keratinocytes and also promote a prompt response in their proliferative capacity [9]. Besides providing this passive temporary surface for cell attachment and proliferation of cells involved in wound healing, they seems to promote angiogenesis and collagen synthesis during this process [10,11]. Importantly, *in vitro* studies suggest that NCMs may to be taken up by macrophages which modify their surface-marker expression to a noninflammatory phenotype and modulate their cytokines production to favor the anti-inflammatory response [9,12]. This point is of a great importance, because one of the characteristic of chronic wounds is the inflammatory stage, where the excess and persistent inflammation prevents correct healing.

Beyond *in vitro* studies, NCMs have already shown to be effective in the treatment of hard-to-heal wounds and ulcers of different etiologies at a clinical level [10,13,14]. However, more studies are required to demonstrate their safety, showing that when used topically NCMs are neither absorbed, nor spread potentially causing undesired side effects. In this sense, special attention must be paid to the macrophages present during the healing process. This type of cells performs multiple beneficial functions during the overall healing process, promoting the transition from the inflammatory to the proliferative phase through production of cytokines and growth factors [15]. However, taking into account that NCM treatment requires daily applications for a variable period of time, and that *in vitro* studies suggest that macrophages take up NCMs, they are likely to be degraded by macrophages present in the wound contributing to potential spread of fragments via the lymphatic pathway [15,16]. Therefore, NCM biodistribution studies are required to ensure that their local effect is restricted to the wound site.

One strategy to study the *in vivo* biodistribution of different nano or microsystems is by labeling with radioisotopes such as technetium-99m (^{99m}Tc), which permits to detect radioactivity in different organs and tissues both through *in vivo* or *ex vivo* techniques [17,18]. ^{99m}Tc is without any doubt the most widely used radionuclide in any nuclear medicine department worldwide. Its availability (as it is easily produced from a commercial ^{99}Mo-^{99m}Tc generator), along with its 140 KeV gamma ray emission and 6-hour half-life make ^{99m}Tc the radioisotope of choice for many clinical imaging procedures. Multiple radiochemical strategies for ^{99m}Tc labeling have been developed in the last 60 years, and many biodistribution studies of different nanosystems using ^{99m}Tc have been published [19–22].

In summary, the aim of this work was to confirm the lack of NCM systemic absorption after topical administration on impaired skin as well as their safety in the treatment of chronic and hard-to-heal wounds. For this, NCM labeling with ^{99m}Tc was optimized to perform *in vivo* biodistribution studies by means SPECT/CT imaging in an open wound rat animal model using a repeated dose experimental design.

2. Materials and methods

2.1. NCM samples

NCMs from a commercial microsphere formulation (PolyHeal® Micro), consisting in negatively charged polystyrene microspheres (4.5 × 10^6 microspheres/mL; 4.5 μm) suspended in 22 % glycerol and phosphate buffer (KH_2PO_4/Na_2HPO_4) in water for injection, were used for all experiments. The commercial formulation was washed with $_{dd}H_2O$, centrifuged at 27.000*g* for 10 min and opportunely re-suspended in $_{dd}H_2O$.

2.2. NCM labeling with [^{99m}Tc]TcO_4^-

NCMs were labeled by a previously reported direct method [21] with technetium-99 m obtained from a ^{99}Mo/^{99m}Tc generator as Na[^{99m}Tc]TcO_4^-). In short, NCMs were labeled by [^{99m}Tc]TcO_4^- reduction with tin chloride in a helium atmosphere. The process was optimized in a series of sequential experiments using different tin chloride concentrations and incubation times for NCM radiolabeling, and then, to evaluate both the specificity and stability of the radiolabel using a DTPA-challenge in saline and human plasma (see Supplementary information).

2.3. Final conditions for NCM labeling with [^{99m}Tc]TcO_4^-

After optimization of the radiolabeling conditions, experiments were carried out using 30 μL of NCMs in aqueous suspension (0.81 mg) that were labeled with 370 MBq of [^{99m}Tc]TcO_4^- using 40 μL of 0.5 mg/ml $SnCl_2$, for 10 min. NCMs were then recollected by centrifugation at 27.000 g for 2 min, washed twice with NaCl 0.9% and resuspended in a volume of vehicle solution (22% glycerol and phosphate buffer in water for injection) to obtain a final concentration of 17.5 μg in 70 μL.

2.4. Biodistribution studies

2.4.1. Animal model

All the procedures involving animals were carried out in accordance with the guidelines of the European Communities Council Directive (2010/63/EU) and the Spanish Government (RD 53/2013) and were approved by the Ethics Committee for Animal Experimentation of the University of Navarra (protocol CEEA/030-17[A]). Twenty-four female Wistar rats (212 ± 22.5 g, Harlan Laboratories) were used. Animals were socially housed on 12 h light–dark cycles under standard conditions in compliance with the current regulation and given free access to food and water. An open wound animal model was created as previously reported [21]. Briefly, surgical full-thickness wounds were created in the upper part of the back using a 10 mm punch biopsy tool under anesthesia. Immediately after wound creation, ^{99m}Tc-NCMs (17.5 μg/animal in 70 μL; 6.5 ± 0.5 MBq; n = 12) or free [^{99m}Tc]TcO_4^- used as control (6.1 ± 0.75 MBq in 70 μL; n = 12) were administered on the wound. Afterwards, wounds were covered with a non-woven gauze and one layer of petrolatum gauze (Tegaderm®, 3 M GmbH) secured with a self-adhesive tape (Hypafix, BSN medical). Half-life of ^{99m}Tc and total administered dose were considered for data analysis.

2.4.2. Experimental design

Animals were divided in two categories depending on the number of administered doses: (A) single and (B) repeated doses, used to study the action of macrophages over NCMs. Fig. 1 shows the experimental conditions and design for *in vivo* and *ex vivo* biodistribution studies. For the single dose condition (1 day), ^{99m}Tc-NCMs or free [^{99m}Tc]TcO4$^-$ were administered at day 0 and SPECT/CT images obtained at 1, 2, 12 and 24 h. After the last image, rats were euthanized using the euthanasia solution T-61 (intravenous injection, 0.3 ml/kg). In the case of the repeated dose group (11 days), ^{99m}Tc-NCMs or free [^{99m}Tc]TcO_4^- were administered at days 0 and 10, while unlabeled NCMs (treated group) or

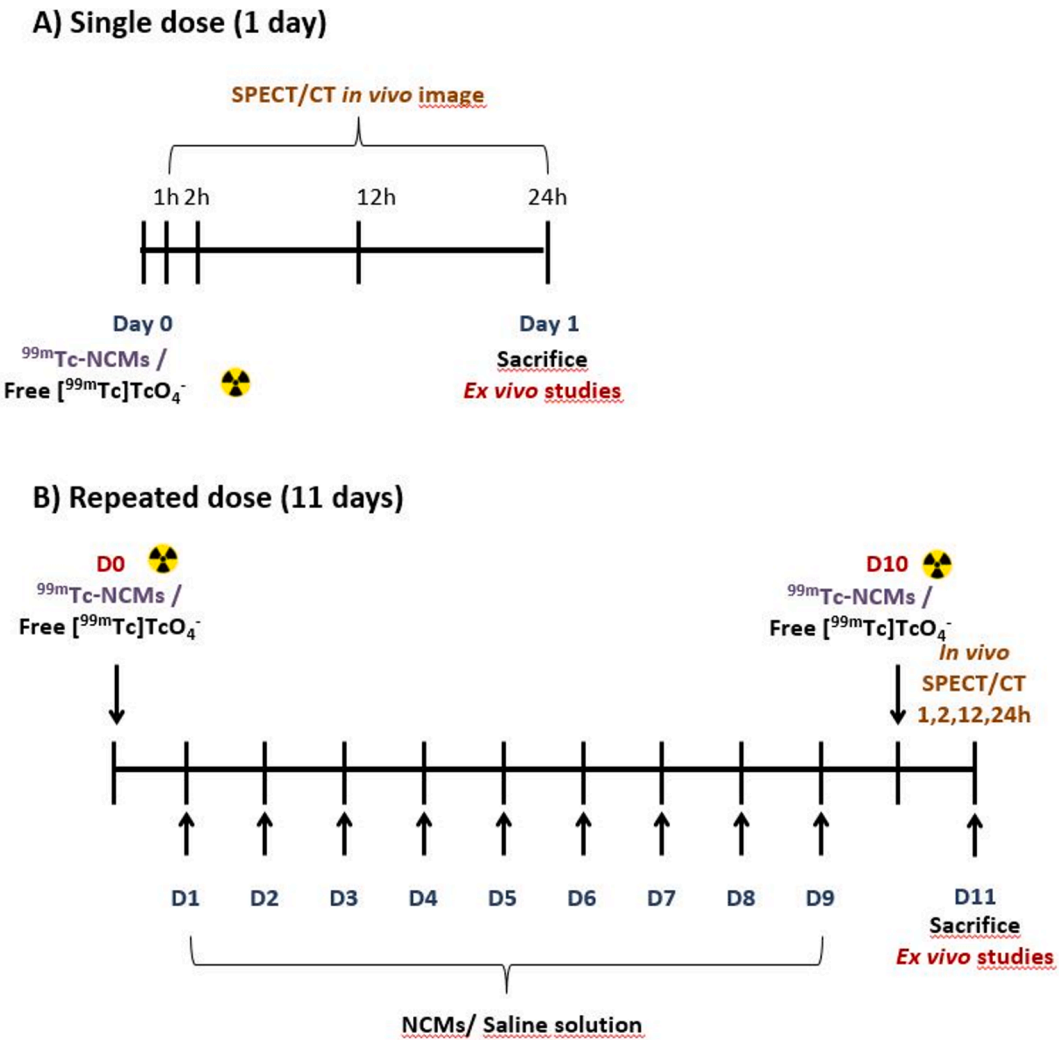

Fig. 1. Experimental conditions and design of biodistribution studies.

saline solution (control group) were administered daily from day 1 to day 9. Finally, SPECT/CT images were obtained at 1, 2, 12 and 24 h of day 11, before rats were euthanized for *ex vivo* studies.

2.4.3. In vivo biodistribution studies by SPECT/CT

SPECT/CT images were acquired using a Symbia T2 TruePoint SPECT-CT system (Siemens). Rats were placed in prone position under inhalation anesthesia with isoflurane (2% in 100% O_2 gas) administered by a respiratory mask. To quantitatively compare the images avoiding the effect of ^{99m}Tc radioactive decay, image acquisition time was increased over the temporal points proportionally to the elapsed ^{99m}Tc time decay. Parameters of the SPECT images were: matrix 128 × 128, 90 images, 7 images per second; and of the CT images: 110 mAs and 130 kV, 130 images, slice thickness 3 mm. Images were reconstructed applying attenuation and dispersion corrections. Fused images were viewed using the Syngo MI Applications TrueD software (Siemens). Following the qualitative analysis, images were exported to the specialized software PMOD v3.2 (PMOD Technologies, Switzerland) for quantitative analysis, which was carried out drawing volumes of interest (VOIs) on CT anatomical images that were then transferred to SPECT images. VOIs of the whole body, wound area, stomach and intestine were drawn. Percentage of the activity in each organ was calculated considering the total dose as the measured activity in the VOI of the total body in the image acquired at 1 h.

2.4.4. Ex vivo biodistribution studies after dissection

The *ex vivo* biodistribution studies were carried out 24 h after administrating ^{99m}Tc-NCMs or free [^{99m}Tc]TcO_4^- (at day 1 and day 11 for single and repeated dose, respectively). After animal euthanasia, the following organs were dissected as a whole: ovaries, kidneys, stomach, small intestine, large intestine, caecum, lung, thyroid, brain, eye, gastrocnemius muscle and axillary nodes. Moreover, samples of liver, skin (abdominal area), blood and urine were taken. To analyze the wound area, skin adjacent to the wound, subcutaneous tissue under the wound corresponding to the fat (*panniculus adiposus*) and muscle tissue under the wound (*panniculus carnosus*) were dissected separately. All tissue and organ samples, together with the dressing (non-woven gauze and Tegaderm®) used in each animal were measured in a gamma counter. Biodistribution was calculated and expressed as a percentage of the total dose per whole-organ (% dose/organ), measuring two equal doses as those administered to the animals in the gamma counter and considering the obtained mean value as total activity. To calculate the activity in blood and whole liver (standard weight of 13.31 g), total blood volume (TBV) was calculated using the following formula [23]: TBV = (0.06 × body weight) + 0.77.

3. Results and discussion

NCMs are proposed as a new biomaterial able to reactivate the wound-healing process in open and hard-to-heal wounds. The aim of this study was to provide relevant information about the safety of NCMs in

relation to their possible systemic absorption after topical administration on skin open wounds performing for the first time a biodistribution study of this compound. For such purpose, NCMs were radiolabeled with ^{99m}Tc, a gamma-emitting radioisotope that allows their detection by means of a SPECT/CT scanner. This novel approach allows longitudinal *in vivo* biodistribution studies in the same animal, helping to evaluate the residence time of NCMs on the wound and the possible accumulation in other organs.

This study is of great importance, since It has previously been demonstrated that macrophages can phagocyte NCMs, inducing a phenotype switch towards a non-inflammatory state [9,12]. However, macrophage migration from the wound site could potentially imply accumulation of NCMs in distant organs/tissues. The proposed biodistribution studies could demonstrate the absence of NCM absorption after topical administration, implying a significant reduction in the potential side effects. These biodistribution studies were carried out evaluating the presence of NCMs in different organs after single and repeated doses in an open-wound rat model after a surgical full-thickness excision on the dorsum. It must be taken into account that no animal model is capable of mimicking the healing processes of chronic wounds due to the anatomical differences of the skin and the physiological processes involved [24]. In our study, the choice of rats is justified by their wide availability and adequate size for *in vivo* imaging. Moreover, within the rat animal models, this specific model is widely used to study chronic wounds [25]. Despite the experimental model has its limitations, it may allow us to obtain useful data to study the *in vivo* biodistribution of NCMs at tissue level.

3.1. NCM radiolabeling

NCMs were radiolabeled with [^{99m}Tc]TcO_4^- by a direct method with high efficiency. The radiolabeling reaction is based on the binding of ^{99m}Tc to negatively charged moieties on the surface of the NCMs. ^{99m}Tc forms strong coordination bonds that finally lead to the formation of stable technetium-labelled structures. In fact, such kind of reaction is the basis of the radiochemistry processes underlying the preparation radiolabeling of many ^{99m}Tc radiopharmaceuticals used in the clinical setting. In our case, consecutive experiments were performed in order to optimize the radiolabeling process and to ensure that radiolabeling was stable. When obtained from the ^{99}Mo/^{99m}Tc generator, ^{99m}Tc is obtained as [^{99m}Tc]TcO_4^-, in which ^{99m}Tc has a 7 + oxidation state, that is extremely stable and non-reactive, so reduction of unreactive Tc(VII) to more reactive technetium species with lower oxidation states (such as Tc (IV)) are needed for efficient radiolabeling. In radiopharmacy practice, the most commonly reducing agent used is $SnCl_2$. However, low concentrations may be insufficient to quantitatively reduce [^{99m}Tc]TcO_4^- while an excess may lead to the formation of ^{99m}Tc-tin colloids [26]. These colloids can form in the presence of a large excess of tin when the reduction capacity of this ion is altered by an oxidant if it were present in the reaction (O_2 excess). Thus, selection of the most suitable $SnCl_2$ concentration is a critical point in the radiolabeling procedure. Our results showed that an optimum radiolabeling (98.42 ± 0.75 %) was achieved using a $SnCl_2$ concentration of 0.5 mg/mL. Decreasing concentrations of $SnCl_2$ rendered poor labeling efficiencies (0.05 mg/mL, 72.9 ± 16.9 %; 0.005 mg/mL, 0.77 ± 0.3 %). Once the optimal concentration of $SnCl_2$ was determined, time required to radiolabel NCMs after [^{99m}Tc]TcO_4^- addition was also studied. Additionally, the presence of ^{99m}Tc-tin colloids in the sample was determined because colloidal impurities could interfere with biodistribution studies that might lead to misinterpretations and erroneous conclusions [27]. In this case, centrifugation was selected as a very efficient and simple way to separate colloids due to the large size of NCMs (4.5 μm) [28]. Data showed that 10 min was enough to achieve an appropriate labeling yield and that the presence of ^{99m}Tc-tin colloids in those conditions was negligible (see Table 1 in Supplementary material). Finally, to simulate the *in vivo* environment and assess radiolabeling stability of NCMs, two different experiments were performed. Firstly, radiolabeling was tested with different DTPA concentrations ("DTPA challenge", Table 2). DTPA is a chelating agent that has high affinity for metal cations and may mimic transchelation of [^{99m}Tc]TcO_4^- that might occur in physiological conditions. Our results showed the high affinity of ^{99m}Tc for this type of NCMs, as very high labeling yields were achieved even in the presence of significant DTPA concentrations (almost 89 % of labeling with DTPA concentrations of 0.1 mM, Table 2A in Supplementary material). In additional experiments, radiolabeling stability was tested *in vitro* after incubation with saline or human serum. Stability was tested up to 24 h post-radiolabeling, as that was the duration of the *in vivo* NCM biodistribution studies. An excellent labeling stability was observed at 24 h both in saline (92.2 % ± 3.6 at 24 h) and human serum (97.3 % ± 2.5 at 24 h) (Table 2B in Supplementary material). Both experiments indicate that radiolabeling was very stable, supporting that the detected signal in the *in vivo* experiments corresponded to ^{99m}Tc-NCMs, and not to other technetium-labeled species that could have been released over time.

3.2. In vivo biodistribution studies by SPECT/CT

^{99m}Tc-NCMs were used for *in vivo* biodistribution studies by SPECT/CT imaging at 1, 2, 12 and 24 h post-administration (Fig. 2). Qualitative analysis of the volumetric images showed that ^{99m}Tc-NCM signal was stable over time on the wound area, demonstrating that NCMs remained on the wound without being absorbed for at least 24 h (Fig. 2A). The same pattern was observed for those animals treated with repeated doses (Fig. 2C). Analysis of the image sections proved that the signal location was on the surface of the animal and not at a lung level (Fig. 2E). Administration of [^{99m}Tc]TcO_4^- on the wound area was used as a negative control, necessary to rule out that the detected signal in the treatment group came from ^{99m}Tc released from the radiolabeled NCMs [18]. Regarding the control animal group, a main difference was observed compared to animals treated with single or repeated doses (Fig. 2C, 2D). A rapid and higher absorption of ^{99m}Tc was detected in the animals treated with a single dose, where an uptake in the stomach was observed in the images around 1 h after administration, and that decreased over time as it moved along the gut. This pattern is compatible with the natural uptake of free [^{99m}Tc]TcO_4^-, which is metabolized by the gastric mucosa [29]. However, control animals with repeated doses showed much lower uptake, probably because the natural healing process on the wound hindered the absorption of free [^{99m}Tc]TcO_4^- administered at day 10.

Results from the quantitative analysis of the SPECT/CT images confirmed the information obtained from the visual analysis (Fig. 2E and 2F). Calculation of the activity percentage was performed in the areas where a clear signal was detected and an accurate VOI could be drawn (wound area, stomach and intestinal area), showing that nearly 100 % of the signal was maintained over time on the wound area in the animals treated with ^{99m}Tc-NCMs with single or repeated doses. Only in those control animals receiving a single dose of free [^{99m}Tc]TcO_4^- a signal displacement was observed over time. A summary of the numeric data obtained from the *in vivo* studies is shown in Table 3 of Supplementary material.

3.3. Ex vivo biodistribution studies using dissection

In addition to these imaging studies, *ex vivo* studies were also carried out at the experiment end-point (24 h post-administration) by dissecting different organs and detecting gamma emission in the tissues with a gamma counter. Due to the extreme sensitivity of these equipments, this technique allows a more detailed study of the biodistribution of compounds at a tissue level of those organs that are difficult to study *in vivo* due to the low uptake or resolution limits of SPECT/CT scanners. Thus, *ex vivo* biodistribution studies are the ideal complement to *in vivo* imaging studies [30,31]. In this study, a large list of organs and samples was studied to rule out the possible dissemination of NCMs from the

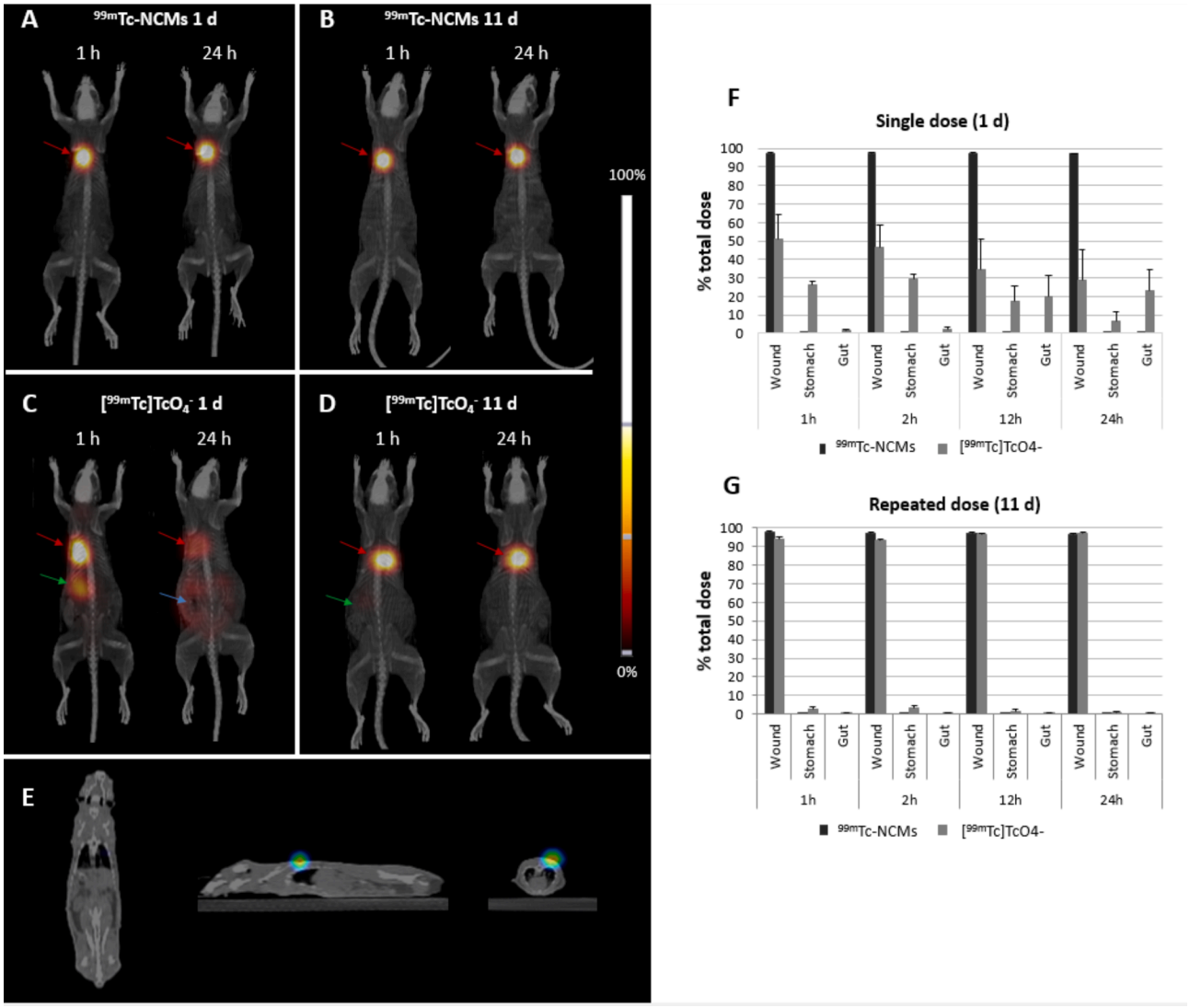

Fig. 2. Volumetric images of the SPECT/CT studies of animals from a single dose group (A, C) or repeated dose group (B, D). Representative images of the same animal are shown at 1 h and 24 h post-administration of ^{99m}Tc-NCMs (A, B) or free ^{99m}TcO4$^-$ (C, D). Red arrows point out the signal at a wound level. Green and blue arrows point to the stomach area and to the intestine respectively. E) Images of sections of the three axes (longitudinal, sagittal and coronal) of a representative animal treated with ^{99m}Tc-NCMs on the wound. Signal was observed on the animal surface without reaching the lungs, although the spillover effect due to limitations of the tomograph resolution caused that part of the signal appeared inside the body. Bar graphs representing quantitative data from SPECT/CT images over time from a single dose group (F) or repeated group (G) (mean ± SD, n = 6). (For interpretation of the references to colour in this figure legend, the reader is referred to the web version of this article.)

wound (Table 1). The physiological phagocytic action of macrophages to remove foreign materials from a wound followed by migration to nearby draining lymph nodes could be an important route for NCM dissemination [9], especially in animals with long lasting treatments (repeated dose). Consequently, it is important to consider the sample of the axillary lymph nodes from Table 1. Such nodes were dissected as they would be the main draining lymph organs from a wound located on the upper back, such as the one in our animal model. In the control animals, different areas of the intestine were dissected (small intestine, large intestine and caecum), as the signal was mainly detected in the digestive system. Finally, the *ex vivo* technique allowed dissecting the wound area in detail (skin, muscle), as well as studying the presence of NCMs in the dressing, an important factor to keep in mind in this type of treatments (Fig. 3) [21]. All these tissues and components were impossible to discriminate in the SPECT/CT images, and were all included in the VOI called "wound".

Ex vivo experiments confirmed that nearly 85 % of the activity was found at the wound level in treated animals (Fig. 3). In animals treated with a single dose, and after having contact with the wound, most of the NCMs were taken away when the dressing was removed (78.07 % ± 5.65), and some NCMs remained in the skin surrounding the wound (6.31 % ± 1.6 %). NCM presence was almost testimonial on the subcutaneous tissue (*panniculus adiposus*, 0.13 % ± 0.11), but was absent on the *panniculus carnosus* (muscle). Presence of NCMs on the wound skin was lower in the animals treated for several days (2.93 % ± 2.40), probably because the wound healing process hindered NCM adsorption as previously discussed. Signal from other organs or tissues was negligible in animals treated with a single dose and nearly undetectable in most cases, even decreasing in animals that received repeated doses (Table 1). Remarkably, no signal was detected in axillary lymph nodes in any of the experimental conditions (single or repeated doses). Although it is not possible to completely rule out the uptake of NCM by macrophages, this fact suggests that there is no massive degradation of NCMs by this cell type at least during the time interval of the experiment.

Taken together, all the data indicate that NCMs remain on the wound area during treatment, and that there is no direct absorption or

Table 1
Ex vivo biodistribution results. Data from the *ex vivo* biodistribution studies correspond to those obtained after sacrifice at 24 h post-administration in animals treated with a single dose (1 day) or repeated doses (11 days). Results are expressed as percentage of the injected dose and were calculated per whole-organ, whenever possible, except from urine and skin samples. Results are showed as mean ± SD (n = 6).

	^{99m}Tc-NCMs 1 day	^{99m}Tc-NCMs 11 days	[^{99m}Tc]TcO_4^- 1 day	[^{99m}Tc]TcO_4^- 11 days
Organs and tissues				
Total blood	0.05 ± 0.03	0.04 ± 0.07	0.25 ± 0.18	0.14 ± 0.25
Skin	0.00 ± 0.00	0.01 ± 0.02	0.01 ± 0.01	0.01 ± 0.01
Muscle	0.00 ± 0.00	0.00 ± 0.00	0.00 ± 0.00	0.00 ± 0.00
Urine	0.10 ± 0.09	0.00 ± 0.00	0.68 ± 0.24	0.03 ± 0.02
Ovaries	0.00 ± 0.00	0.00 ± 0.00	0.00 ± 0.00	0.00 ± 0.00
Spleen	0.00 ± 0.00	0.00 ± 0.00	0.01 ± 0.00	0.00 ± 0.00
Kidneys	0.31 ± 0.21	0.01 ± 0.01	1.08 ± 0.62	0.14 ± 0.0.05
Stomach	0.09 ± 0.04	0.00 ± 0.01	6.55 ± 3.07	1.07 ± 0.75
Small intestine	0.05 ± 0.03	0.00 ± 0.00	1.36 ± 0.48	0.13 ± 0.07
Large intestine	0.08 ± 0.04	0.01 ± 0.01	4.79 ± 2.04	0.44 ± 0.30
Caecum	0.06 ± 0.04	0.00 ± 0.00	5.33 ± 1.93	0.57 ± 0.28
Liver	0.03 ± 0.02	0.00 ± 0.00	0.35 ± 0.07	0.07 ± 0.03
Lungs	0.00 ± 0.00	0.00 ± 0.00	0.02 ± 0.01	0.00 ± 0.00
Thyroid	0.00 ± 0.00	0.00 ± 0.00	0.02 ± 0.01	0.00 ± 0.00
Brain	0.00 ± 0.00	0.00 ± 0.00	0.00 ± 0.00	0.00 ± 0.00
Eye	0.00 ± 0.00	0.00 ± 0.00	0.00 ± 0.00	0.00 ± 0.00
Axillary lymph nodes	0.00 ± 0.00	0.00 ± 0.00	0.00 ± 0.00	0.00 ± 0.00

degradation. Different topical treatments studied by radiolabeling have shown a variable degree of absorption, probably due to the chemical nature of the product and its size [21,32]. In our case, the large size of the NCMs and their surface charge can favor their retention in the dressing, despite remaining in contact with the wound throughout the treatment. Absorption of [^{99m}Tc]TcO_4^- was higher in animals receiving a single dose of free [^{99m}Tc]TcO_4^- immediately after wound creation. In this case, only 12.9 % of signal retention was observed at the dressing, while the highest signal was detected in organs associated with the digestive system. Noteworthy, in these animals a large part of the dose was not detected, as after 24 h an important part of the radioactivity was probably eliminated in the feces. In control animals receiving repeated doses, an important increase in the signal from the dressing (up to 68.8 %) was observed, and a lower [^{99m}Tc]TcO_4^- presence in other organs, probably because the wound healing process hindered its absorption.

4. Conclusions

NCM labeling with [^{99m}Tc]TcO_4^- was achieved in an easy and effective manner. ^{99m}Tc-NCMs were obtained in high yield, with high radiochemical purity (>99 %) and radiolabeling was stable over time both in saline and human serum. Data from *in vivo* biodistribution studies (SPECT/CT images) revealed excellent retention of NCMs on the wound area for at least 24 h after product administration, both for single and repeated doses. Roughly 100 % of the radioactivity remained on the wound area and no signal was detected in other areas of the body. *Ex vivo* studies revealed that, after being in contact with the wound, most of the NCMs were removed with dressing changes, and only a small proportion remained on the skin surrounding the wound. No activity in lymph nodes was found during repeated administration suggesting absence of phagocytosis exerted by macrophages and their subsequent migration. In conclusion, no systemic absorption was found on the wound either after single or multiple administrations of NCMs. As a whole, our results validate NCMs as safe for local treatment of chronic and hard-to-heal wounds.

Declaration of Competing Interest

The authors declare the following financial interests/personal relationships which may be considered as potential competing interests: 10% of BioKeralty Research Institute AIE belongs to Praxis Pharmaceutical, which possesses the sale license of PolyHeal® Micro. No author

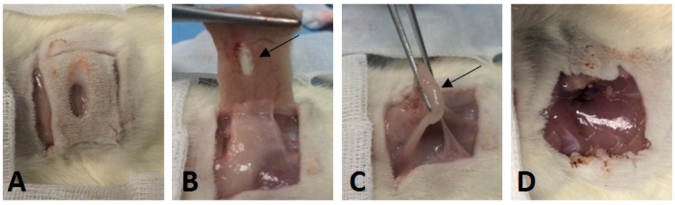

	^{99m}Tc-NCM 1 d	^{99m}Tc-NCM 11 d	[^{99m}Tc]$TcO4^-$ 1 d	[^{99m}Tc]$TcO4^-$ 11 d
Dressing	78.07 ± 5.62	82.11 ± 6.18	12.89 ± 10.63	68.82 ± 6.18
Wound skin	6.31 ± 1.06	2.93 ± 2.40	4.73 ± 3.23	11.38 ± 5.73
Subcutaneous	0.13 ± 0.11	0.01 ± 0.01	0.09 ± 0.04	0.00 ± 0.01
Wound muscle	0.00 ± 0.00	0.00 ± 0.00	0.00 ± 0.00	0.00 ± 0.00

Fig. 3. Procedure to dissect the wound area to obtain tissue samples for the gamma counter. (A-B) Cut of skin surrounding the wound area. The arrow in picture B points to tissue sample corresponding to skin. (C) Subcutaneous tissue (*panniculus adiposus*) sample taking. (D) View of the muscle under the wound area (*panniculus carnosus*) used for counting in the gamma counter. Table shows *ex vivo* counting data expressed as percentage of injected dose (mean ± SD, n = 6).

had control on the results of the assays. The authors have no other conflicts of interest that are directly relevant to the content of this manuscript, which remains their sole responsibility.

Acknowledgments

This project was partially supported by the Basque Government (HAZITEK, ZE-2017/00014) and co-funded by the European Regional Development Fund (ERDF).

Appendix A. Supplementary material

Supplementary data to this article can be found online at https://doi.org/10.1016/j.ejpb.2022.06.001.

References

[1] G. Broughton, J.E. Janis, C.E. Attinger, The basic science of wound healing, Plast. Reconstr. Surg. 117 (SUPPLEMENT) (2006) 12S–34S.
[2] W.H. Eaglstein, V. Falanga, Chronic wounds, Surg. Clin. North Am. 77 (1997) 689–700, https://doi.org/10.1016/S0039-6109(05)70575-2.
[3] G. Han, R. Ceilley, Chronic Wound Healing: A Review of Current Management and Treatments, Adv. Ther. 34 (2017) 599–610, https://doi.org/10.1007/s12325-017-0478-y.
[4] K. Las Heras, M. Igartua, E. Santos-Vizcaino, R.M. Hernandez, Chronic wounds: Current status, available strategies and emerging therapeutic solutions, J. Control. Release. 328 (2020) 532–550, https://doi.org/10.1016/J.JCONREL.2020.09.039.
[5] M.E. Ogle, C.E. Segar, S. Sridhar, E.A. Botchwey, Monocytes and macrophages in tissue repair: Implications for immunoregenerative biomaterial design, Exp. Biol. Med. 241 (2016) 1084–1097, https://doi.org/10.1177/1535370216650293.
[6] S.A. Shah, M. Sohail, S. Khan, M.U. Minhas, M. de Matas, V. Sikstone, Z. Hussain, M. Abbasi, M. Kousar, Biopolymer-based biomaterials for accelerated diabetic wound healing: A critical review, Int. J. Biol. Macromol. 139 (2019) 975–993, https://doi.org/10.1016/j.ijbiomac.2019.08.007.
[7] Y. Feng, M. Borrelli, T. Meyer-ter-Vehn, S. Reichl, S. Schrader, G. Geerling, Epithelial Wound Healing on Keratin Film, Amniotic Membrane and Polystyrene In Vitro, Curr. Eye Res. 39 (2014) 561–570, https://doi.org/10.3109/02713683.2013.853804.
[8] D. Khatua, B. Kwak, K. Shin, J.-M. Song, J.-S. Kim, J.-H. Choi, Influence of charge densities of randomly sulfonated polystyrene surfaces on cell attachment and proliferation, J. Nanosci. Nanotechnol. 11 (2011) 4227–4230, https://doi.org/10.1166/jnn.2011.3675.
[9] E. Santos-Vizcaino, A. Salvador, C. Vairo, I. M, R. Hernandez, L. Correa, L. Villullas, G. Gainza, Overcoming the Inflammatory Stage of Non-Healing Wounds: In Vitro Mechanism of Action of Negatively Charged Microspheres (NCMs), Nanomater. 10 (2020) 1–14. 10.3390/NANO10061108.
[10] Y. Shoham, L. Kogan, J. Weiss, E. Tamir, Y. Krieger, Y. Barnea, E. Regev, D. Vigoda, N. Haikin, A. Inbal, O. Arnon, A. Bogdanov-Berezovsky, E. Silberstein, N. Rosenberg, J. Govrin-Yehudain, G. Zeilig, Wound 'dechronification' with negatively-charged polystyrene microspheres: a double-blind RCT, J Wound Care 22 (3) (2013) 144–155.
[11] H. Sorg, D.J. Tilkorn, S. Hager, J. Hauser, U. Mirastschijski, Skin Wound Healing: An Update on the Current Knowledge and Concepts, Eur. Surg. Res. 58 (2017) 81–94, https://doi.org/10.1159/000454919.
[12] W.G. Brodbeck, Y. Nakayama, T. Matsuda, E. Colton, N.P. Ziats, J.M. Anderson, Biomaterial surface chemistry dictates adherent monocyte/macrophage cytokine expression in vitro, Cytokine. 18 (2002) 311–319, https://doi.org/10.1006/cyto.2002.1048.
[13] J.L. Lázaro-Martínez, Y. García-Álvarez, F.J. Álvaro-Afonso, E. García-Morales, I. Sanz-Corbalán, R.J. Molines-Barroso, Hard-to-heal diabetic foot ulcers treated using negatively charged polystyrene microspheres: A prospective case series, J. Wound Care. 28 (2019) 104–109. 10.12968/jowc.2019.28.2.104.
[14] J. Govrin, K. Leonid, E. Luger, J. Tamir, G. Zeilig, R. Shafir, New method for treating hard-to-heal wounds: Clinical experience with charged polystyrene microspheres, Wounds UK 6 (2010) 52–61.
[15] S.K. Brancato, J.E. Albina, Wound macrophages as key regulators of repair: Origin, phenotype, and function, Am. J. Pathol. 178 (2011) 19–25, https://doi.org/10.1016/j.ajpath.2010.08.003.
[16] R.J. Snyder, J. Lantis, R.S. Kirsner, V. Shah, M. Molyneaux, M.J. Carter, Macrophages: A review of their role in wound healing and their therapeutic use, Wound Repair Regen. 24 (2016) 613–629, https://doi.org/10.1111/wrr.12444.
[17] D.S. Lee, H.J. Im, Y.S. Lee, Radionanomedicine: Widened perspectives of molecular theragnosis, Nanomedicine Nanotechnology, Biol. Med. 11 (2015) 795–810, https://doi.org/10.1016/j.nano.2014.12.010.
[18] D. Psimadas, P. Bouziotis, P. Georgoulias, V. Valotassiou, T. Tsotakos, G. Loudos, Radiolabeling approaches of nanoparticles with 99mTc, Contrast Media Mol. Imaging. 8 (2013) 333–339, https://doi.org/10.1002/cmmi.1530.
[19] R. Ramos-Membrive, Á. Erhard, I. Luis de Redín, G. Quincoces, M. Collantes, M. Ecay, J.M. Irache, I. Peñuelas, In vivo SPECT-CT imaging and characterization of technetium-99m-labeled bevacizumab-loaded human serum albumin pegylated nanoparticles, J. Drug Deliv. Sci. Technol. 64 (2021), 101809, https://doi.org/10.1016/J.JDDST.2020.101809.
[20] S. Dos Reis, S. Pinto, F. de Menezes, R. Martinez-Manez, E. Ricci-Junior, L. Alencar, E. Helal-Neto, A. da Silva, P. de Barros, R.-O. Lisboa, Senescence and the Impact on Biodistribution of Different Nanosystems: the Discrepancy on Tissue Deposition of Graphene Quantum Dots, Polycaprolactone Nanoparticle and Magnetic Mesoporous Silica Nanoparticles in Young and Elder Animals, Pharm. Res. 37 (2020), https://doi.org/10.1007/S11095-019-2754-9.
[21] C. Vairo, M. Collantes, G. Quincoces, S. Villullas, I. Peñuelas, M. Pastor, A.G. Gil, E. Gainza, R.M. Hernandez, M. Igartua, G. Gainza, Preclinical safety of topically administered nanostructure lipid carriers (NLC) for wound healing application: biodistribution and toxicity studies, Int. J. Pharm. 569 (2019), https://doi.org/10.1016/j.ijpharm.2019.118484.
[22] M. Lopes, D. Aniceto, M. Abrantes, S. Simões, F. Branco, I. Vitória, M. Botelho, R. Seiça, F. Veiga, A. Ribeiro, In vivo biodistribution of antihyperglycemic biopolymer-based nanoparticles for the treatment of type 1 and type 2 diabetes, Eur. J. Pharm. Biopharm. 113 (2017) 88–96, https://doi.org/10.1016/J.EJPB.2016.11.037.
[23] H.B. Lee, M.D. Blaufox, Blood volume in the rat, J. Nucl. Med. 26 (1985) 72–76.
[24] A. Grada, J. Mervis, V. Falanga, Research Techniques Made Simple: Animal Models of Wound Healing, J. Invest. Dermatol. 138 (2018) 2095–2105.e1, https://doi.org/10.1016/j.jid.2018.08.005.
[25] W.A. Dorsett-Martin, Rat models of skin wound healing: A review, Wound Repair Regen. 12 (2004) 591–599, https://doi.org/10.1111/j.1067-1927.2004.12601.x.
[26] Z. He, X. Zhang, J. Huang, Y. Wu, X. Huang, J. Chen, J. Xia, H. Jiang, J. Ma, J. Wu, Immune activity and biodistribution of polypeptide K237 and folic acid conjugated amphiphilic PEG-PLGA copolymer nanoparticles radiolabeled with 99mTc, Oncotarget 7 (47) (2016) 76635–76646.
[27] N. Geskovski, S. Kuzmanovska, M. Simonoska Crcarevska, S. Calis, S. Dimchevska, M. Petrusevska, P. Zdravkovski, K. Goracinova, Comparative biodistribution studies of technetium-99 m radiolabeled amphiphilic nanoparticles using three different reducing agents during the labeling procedure, J. Label. Compd. Radiopharm. 56 (2013) 689–695, https://doi.org/10.1002/jlcr.3097.
[28] A. Desbrée, T. Bonnard, E. Blanchardon, A. Petiet, D. Franck, C. Chauvierre, C. Le Visage, Evaluation of Functionalized Polysaccharide Microparticles Dosimetry for SPECT Imaging Based on Biodistribution Data of Rats, Mol. Imaging Biol. 17 (2015) 504–511, https://doi.org/10.1007/s11307-014-0812-6.
[29] S.A. Emamian, E. Shalaby-Rana, M. Majd, The spectrum of heterotopic gastric mucosa in children detected by Tc-99m pertechnetate scintigraphy, Clin. Nucl. Med. 26 (2001) 529–535, https://doi.org/10.1097/00003072-200106000-00010.
[30] E.A. Fragogeorgi, I.N. Savina, T. Tsotakos, E. Efthimiadou, S. Xanthopoulos, L. Palamaris, D. Psimadas, P. Bouziotis, G. Kordas, S. Mikhalovsky, M. Alavijeh, G. Loudos, Comparative in vitro stability and scintigraphic imaging for trafficking and tumor targeting of a directly and a novel 99mTc (I)(CO)3 labeled liposome, Int. J. Pharm. 465 (2014) 333–346, https://doi.org/10.1016/j.ijpharm.2014.01.042.
[31] P. Areses, M.T. Agüeros, G. Quincoces, M. Collantes, J.Á. Richter, L.M. López-Sánchez, M. Sánchez-Martínez, J.M. Irache, I. Peñuelas, Molecular imaging techniques to study the biodistribution of orally administered (99m)Tc-labelled naive and ligand-tagged nanoparticles, Mol. Imaging Biol. 13 (2011) 1215–1223, https://doi.org/10.1007/s11307-010-0456-0.
[32] G.G. Pereira, R. Santos-Oliveira, M.S. Albernaz, D. Canema, G. Weismüller, E. B. Barros, L. Magalhães, M.H.M. Lima-Ribeiro, A.R. Pohlmann, S.S. Guterres, Microparticles of Aloe vera/vitamin E/chitosan: Microscopic, a nuclear imaging and an in vivo test analysis for burn treatment, Eur. J. Pharm. Biopharm. 86 (2014) 292–300, https://doi.org/10.1016/j.ejpb.2013.10.011.